New Journal of Physics
The open access journal at the forefront of physics

Deutsche Physikalische Gesellschaft DPG
IOP Institute of Physics

Published in partnership with: Deutsche Physikalische Gesellschaft and the Institute of Physics

OPEN ACCESS

RECEIVED
26 August 2014

ACCEPTED FOR PUBLICATION
25 November 2014

PUBLISHED
9 January 2015

PAPER

Enhanced nematic and antiferromagnetic phases in the spin-fermion model for strained iron pnictides

Minghui Qin[1,2], **Shuai Dong**[3], **Junming Liu**[2,4] **and Zhifeng Ren**[1]

[1] Department of Physics and TcSUH, University of Houston, Houston, Texas 77204, USA
[2] Institute for Advanced Materials and Laboratory of Quantum Engineering and Quantum Materials, South China Normal University, Guangzhou 510006, People's Republic of China
[3] Department of Physics, Southeast University, Nanjing 211189, People's Republic of China
[4] Laboratory of Solid State Microstructures, Nanjing University, Nanjing 210093, People's Republic of China
E-mail: zren@uh.edu

Keywords: iron-based superconductors, strain effect, phase transition, spin-fermion model

Abstract

The effects of anisotropic superexchange and Fe–Fe hoppings on phase transitions in the undoped three-orbital spin-fermion model are investigated to understand the experimentally reported strain effect in $BaFe_2As_2$. Monte Carlo simulated phase diagrams show that both the collinear antiferromagnetic and nematic transitions shift toward high temperature with the increasing magnitude of anisotropies, qualitatively consistent with experimental observation. Thus, both the anisotropic superexchange and Fe–Fe hoppings are suggested to be responsible for the variation of the transition temperatures of $BaFe_2As_2$ with uniaxial stress. In addition, we observed a 90 degree rotation of the collinear antiferromagnetic order, accompanied with a reversal of the orbital occupancy at the Fermi surface when the sign of the superexchange anisotropy changes, further supporting previous predictions by first principles calculation.

1. Introduction

In the past few years, numerous phase transitions in iron-based superconductors have attracted broad research interest both experimentally and theoretically [1–3]. Experimentally, the long range collinear antiferromagnetic (AFM) order with a wave vector $(\pi, 0)$ (depicted in figure 1(a)) is stabilized at low temperatures (T) in undoped and underdoped iron pnictides, and universally accompanied with an orthorhombic lattice distortion with a longer lattice constant along the AFM direction (the x-axis in figure 1(a)). The structural (tetragonal to orthorhombic) and AFM transitions are closely related, and the former transition temperature T_S is either equal to or slightly higher than the AFM transition temperature T_N: $T_S \geqslant T_N$ [4, 5]. To understand these results, the nematic order is suggested to be developed before the stabilization of the long range AFM order, which drives the structural transition, although no consensus has been reached so far [6–8]. In addition, the possible origin of the nematic state has been theoretically investigated from various approaches, and the biquadratic interaction is believed to play an important role [9–11].

Recent experiments have also demonstrated the significant influence of uniaxial pressure on both the structural and magnetic transitions in iron pnictides [12–14]. Specifically, both of these transitions in $BaFe_2As_2$ shift toward high T when a compressive stress is applied along the shorter axis, as revealed in neutron scattering experiments. Several theoretical attempts have been made to understand this fascinating phenomenon [15–17] For example, the magneto-elastic model has been proposed to study the variation of transition temperatures with uniaxial stress, which qualitatively reproduces the experimental results. It is suggested that magneto-elastic coupling can make the AFM bonds longer than the ferromagnetic (FM) ones in the magnetic state, and in turn results in a change of the transition temperatures under uniaxial strain [15]. In addition, the classical Heisenberg spin model for iron pnictides has been analytically studied using the effective classical field theory. From the pure magnetically driven electronic nematicity point of view, the experimental results can also be well reproduced [16]. Most recently, the effects of uniaxial stress in $BaFe_2As_2$ and $CaFe_2As_2$ were investigated based on density

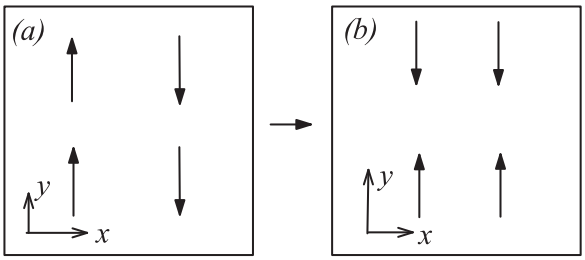

Figure 1. A schematic depiction of the transition from (a) the $(\pi, 0)$ AFM order to (b) the $(0, \pi)$ AFM order. The difference of the lattice constants is exaggeratedly shown here by the x and y coordinates.

functional theory and the phenomenological Ginzburg–Landau model. It is predicted that the FM and AFM directions can be interchanged (the $(\pi, 0)$ AFM state is replaced by $(0, \pi)$, as shown in figure 1), and the orbital occupancies at the Fermi surface are reversed at the critical uniaxial stress when the sign of the orthorhombicity is changed. This phenomenon can be qualitatively understood from the competition between the magneto-elastic coupling and the applied stress [17].

All of these examples help us to understand the physics in iron pnictides to some extent. However, only the localized spins are considered in the models referred above, while the role of itinerant electrons, which is essential for understanding some experimental phenomena (the anisotropy of electrical transport, as an example), is completely ignored [18]. In fact, the itinerant character of electrons should not simply be ignored because most of these iron pnictides are metallic. Fortunately, the spin-fermion (SF) model, in which both itinerant electrons and localized spins are included, has been proposed to simulate pnictide superconductors [19, 20], and the initial calculations have demonstrated the great success of this model for explaining the complicated physics in these systems [21–23]. More interestingly, the SF models are rather similar to the double-exchange model for manganites, allowing one to naturally transfer the research techniques used in the study of manganites to that of iron pnictides [24]. For example, the exchange anisotropies are emphasized in the double-exchange model to simulate the features of the strained manganite thin films, and are suggested to be responsible for the anisotropic resistivities [25]. Naturally, one may expect to use a similar technique to study strained $BaFe_2As_2$. As a matter of fact, a strong anisotropy of the nearest-neighbor (NN) exchange in the magnetic state has been experimentally reported in iron superconductors [26, 27]. Moreover, the magnitude of anisotropy should be changed with the variation of lattice distortion under applied uniaxial stress. However, a detailed theoretical study of the effects of the superexchange and Fe–Fe hopping anisotropies on the phase transitions in strained $BaFe_2As_2$ is not currently available, although the anisotropic exchange coupling has been considered in some of the earlier classical magnetic models without considering the itinerant characters [28, 29].

Therefore, we study the modified three-orbital SF model using the Monte Carlo (MC) method in order to understand the phase transitions in strained $BaFe_2As_2$. The experimentally reported variation of the transition temperatures under uniaxial stress can be qualitatively reproduced when the superexchange and itinerant Fe–Fe hopping anisotropies are taken into account. In addition, it is observed that the FM and AFM directions are switched, accompanied by a reversal of the orbital occupancy at the Fermi surface when the sign of the superexchange anisotropy changes as a result of the sign-change in orthorhombicity, confirming earlier first principles prediction.

2. Model and method

The modified SF model Hamiltonian can be given by:

$$\begin{aligned} H = &- \sum_{i,j}^{\sigma,\alpha,\beta} t_{\alpha,\beta}^{\vec{r}} \left(c_{i,\alpha,\sigma}^{\dagger} c_{j,\beta,\sigma} + h.\,c. \right) - J_{\mathrm{Hund}} \sum_{i} \vec{S}_i \cdot \vec{\sigma}_i \\ &+ \sum_{\langle ij \rangle} J_{NN}^{\vec{r}} \vec{S}_i \cdot \vec{S}_j + J_{NNN} \sum_{[ik]} \vec{S}_i \cdot \vec{S}_k \\ &- J_{\mathrm{Bi}} \sum_{\langle ij \rangle} \left(\vec{S}_i \cdot \vec{S}_j \right)^2 \end{aligned} \tag{1}$$

The first term denotes the Fe–Fe hoppings of itinerant electrons with fermion spin σ in the d_{xz}, d_{yz} or d_{xy} orbitals. $c_{i,\alpha,\sigma}^{\dagger}$ ($c_{i,\alpha,\sigma}$) creates (annihilates) an electron at orbital α of site i. Here, both NN and diagonal next-nearest-neighbor (NNN) hoppings are considered, and the hopping amplitudes are set as (t_1, t_2, t_3, t_4, t_5, t_6, t_7, t_8) = (0.02, 0.06, 0.03, −0.01, −0.2, 0.3, −0.2, −0.1) in units of eV, the same as previous reports (the detailed

mathematical forms can be found in equations (1)–(3) of [30]). In addition, the energy difference between the d_{xy} and the degenerate d_{xz}/d_{yz} orbitals Δ_{xy} is set to be 0.4 eV, and the average itinerant electron density used here is chosen as 4/3. The second term is the Hund interaction between the localized spin S and the itinerant-fermion at site i with coupling $J_{\rm Hund} = 0.1$ eV. The third term is the AFM superexchange interaction between NN localized spins with $J_{NN} = 0.015$ eV, and the fourth term is that between NNN localized spins with coupling $J_{NNN} = 0.01$ eV. At last, the biquadratic interaction $J_{\rm Bi} = 0.003$ eV between NN localized spins is also considered because this term is suggested to be very important for the nematic order and cannot be neglected in any models for pnictide superconductors [31].

It is expected that a compressive stress applied along the shorter axis will further enhance the orthorhombic distortion, and in turn enhance the anisotropy of the NN superexchange interaction [29]. Thus, the influence of the anisotropy of the NN superexchange interaction on the phase transitions is investigated in order to simulate the effect of the uniaxial stress reported in experiments. Here, a parameter $A_J = J^x_{NN}/J^y_{NN} - 1$ (satisfying the constraint $J^x_{NN} + J^y_{NN} = 2J_{NN}$) is defined to characterize the degree of the NN superexchange anisotropy. On the other hand, the NN Fe–Fe hopping amplitudes (t_1, t_2, t_5, and t_7) could also become anisotropic in the strained system. Up to now, a clear relation between the Fe–Fe hoppings and lattice constant is not available [32], and as a first order approximation the anisotropies of the Fe–Fe hoppings between different orbitals are simply characterized by $A_t = t^x_{NN}/t^y_{NN} - 1$ with the constraint of $t^x_{NN} + t^y_{NN} = 2t_{NN}$ which is orbital-independent, as for strained manganites [25]. Moreover, both the NNN superexchange interaction and Fe–Fe hoppings are less affected by the applied stress, and their anisotropies are not considered in this work.

The above Hamiltonian at finite T was studied via a well-known MC method on a two-dimensional 8×8 lattice with periodic boundary conditions [24]. In the simulation, the first 10^4 MC steps are used for thermal equilibrium and another 2×10^4 MC steps are used for measurements. To illustrate the development of the collinear AFM orders, the spin structure factor Φ is calculated [33]. On the other hand, the spin nematic order parameter can be defined as: [34]

$$\Psi = \left| \frac{1}{2N} \sum_i \left(\vec{S}_i \cdot \vec{S}_{i+x} - \vec{S}_i \cdot \vec{S}_{i+y} \right) \right|, \tag{2}$$

where N is the number of sites. At last, the magnetic susceptibility χ_Φ and the nematic susceptibility χ_Ψ are also calculated to estimate the magnetic and nematic transition temperatures $T_{\rm N}$ and $T_{\rm S}$, respectively.

3. Results and discussion

As discussed above, the NN superexchange anisotropy should be enhanced further when a compressive stress is applied along the FM (shorter bonds) direction. Thus, the effect of positive A_J on the phase transitions is investigated, and the corresponding results are given in figure 2. First, the anisotropy of the Fe–Fe hoppings is not taken into account ($A_t = 0$) to clarify the role of A_J. When T falls down to the critical point (~118 K for $A_J = 0.14$), $\Phi(\pi, 0)$, the spin structure factor at the wave vector $(\pi, 0)$ increases from the background baseline, fingering the development of the $(\pi, 0)$ AFM order. The AFM transition temperatures for various A_J can be estimated from the positions of the peaks in $\chi_{\Phi(\pi,0)}$, as shown in figure 2(b). It is clearly shown that the AFM transition shifts toward higher T as A_J increases, indicating that the $(\pi, 0)$ AFM order can be further enhanced by the superexchange anisotropy. In addition, a similar effect of A_J on the nematic transition has also been observed in our simulations. The nematic transition points for various A_J are estimated from the calculated Ψ and χ_Ψ, as given in figures 2(c) and (d), respectively. It is clearly shown that the transition from the paramagnetic (PM) order to the nematic one occurs at a higher temperature for a larger A_J.

The enhancements of the AFM and nematic orders with increasing A_J may be qualitatively understood from the energy landscape. On one hand, in such a frustrated spin system, the collinear AFM and nematic orders can be developed due to strong competition between the NN and NNN AFM exchange interactions [35]. On the other hand, the energy gain from the NN exchange interaction due to the transition from the PM order to the nematic one increases quickly as A_J increases. At the same time, the variation of the other couplings in this transition is almost independent on A_J. Consequently, the effective couplings in the $(\pi, 0)$ AFM and nematic orders are enhanced by positive A_J and stronger thermal fluctuations are needed to break these two orders, resulting in the increases of $T_{\rm N}$ and $T_{\rm S}$. As a result, it is observed that both the $(\pi, 0)$ AFM and nematic transitions shift toward the higher T with increasing A_J, qualitatively consistent with the experimental report on strained $BaFe_2As_2$. Furthermore, the separations between $T_{\rm S}$ and $T_{\rm N}$ ($T_{\rm S} > T_{\rm N}$) are observed for all A_J, indicating that the nematic order can be developed in advance of the AFM order. The stabilization of the nematic state above $T_{\rm N}$ may be due to the positive biquadratic interaction, as systematically discussed in our earlier work [23].

Subsequently, we paid attention to the effect of the Fe–Fe hoppings anisotropy A_t on the phase transitions in iron pnictides. The study in this part is based on the simplified assumption that all the NN hoppings (t_1, t_2, t_5,

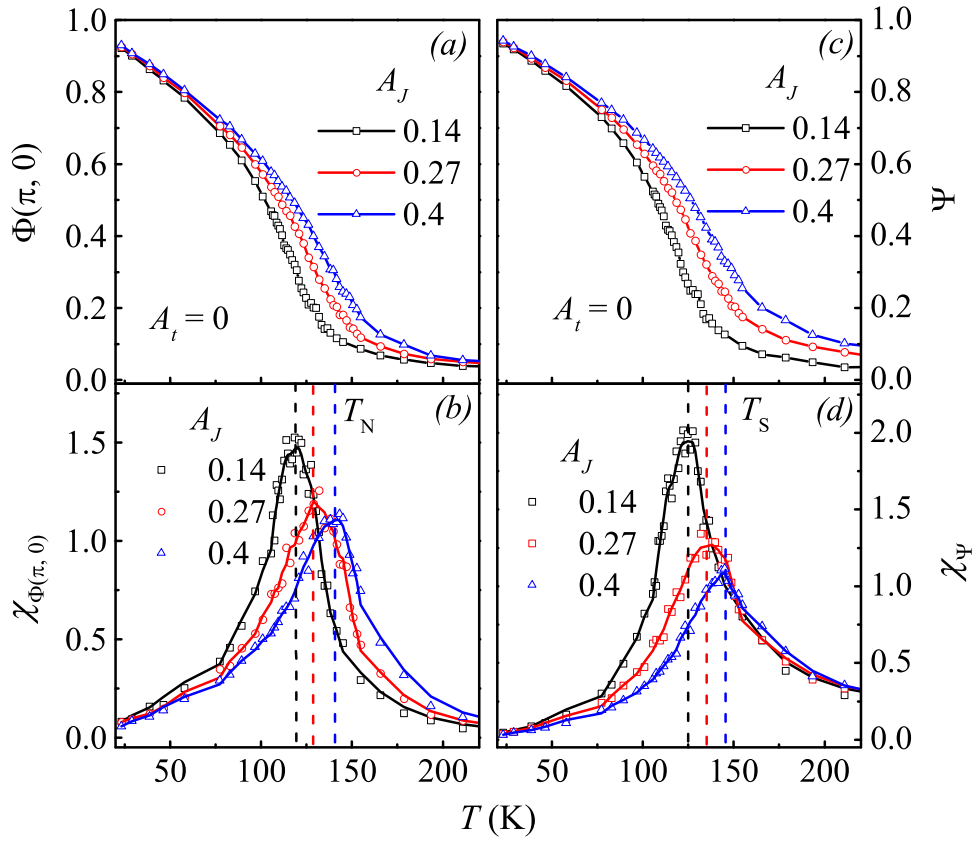

Figure 2. Calculated $\Phi(\pi, 0)$ (a) and its susceptibility $\chi_{\Phi(\pi,0)}$ (b), Ψ (c) and χ_Ψ (d) as a function of T at $A_t = 0$ for various positive values of A_J.

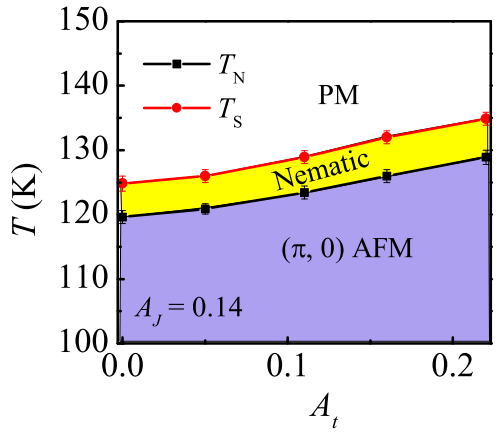

Figure 3. The phase diagram in the (A_t, T) plane at $A_J = 0.14$.

and t_7) change with the lattice constant or Fe–As–Fe angles in the same way. In addition, a small positive $A_J = 0.14$ is considered here to provide a bias field to avoid multi-axes of magnetic domains [36]. The simulated results are summarized in figure 3 which shows the simulated phase diagram in the (A_t, T) parameter space. It is observed that both T_N and T_S slowly increase with the increase of A_t, demonstrating that both the AFM and nematic orders are also favored by the anisotropy of the Fe–Fe hoppings. However, one may note that the variation of the transition temperatures due to A_t is much smaller than that caused by the same valued A_J. Thus, our simulations suggest that the effect of the anisotropic Fe–Fe hopping on the phase transitions in strained pnictides is much weaker than that of the anisotropic superexchange, in contrast to the case of stained manganites.

So, in this work, we found that both anisotropic superexchange and Fe–Fe hopping are partly responsible for the experimentally reported variation of the magnetic and structural transition temperatures of $BaFe_2As_2$ with

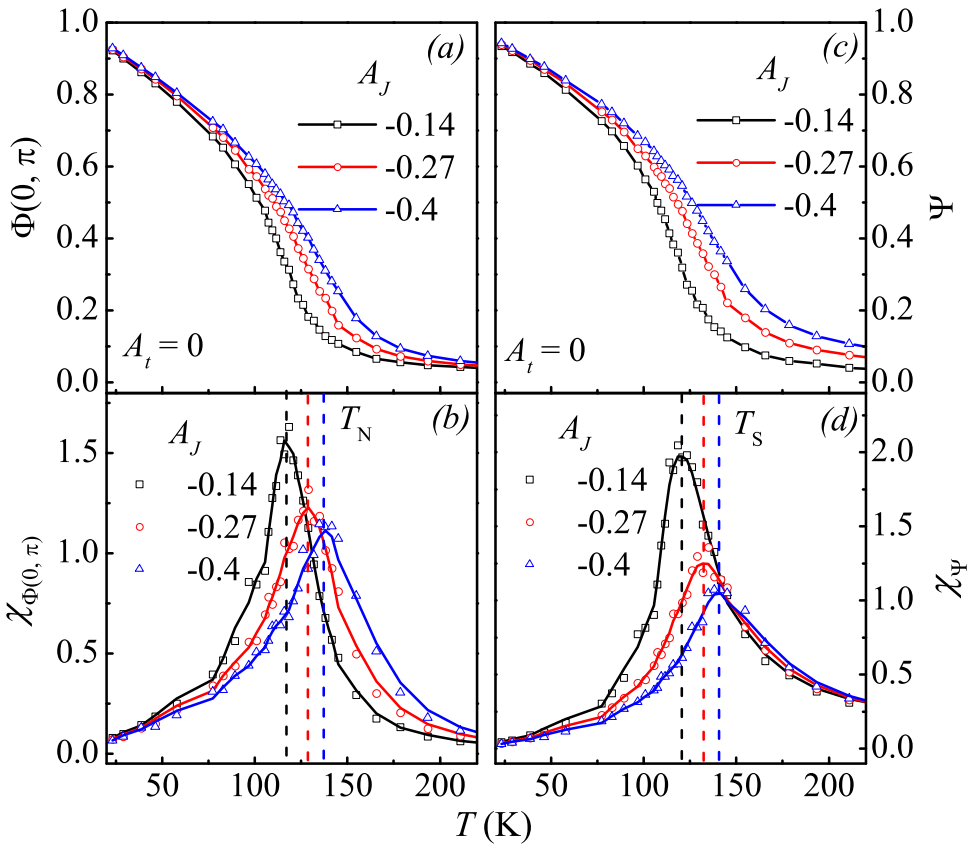

Figure 4. Calculated $\Phi(0, \pi)$ (a) and its susceptibility $\chi_{\Phi(0,\pi)}$ (b), Ψ (c) and χ_Ψ (d) as a function of T at $A_t = 0$ for various negative values of A_J.

external uniaxial stress. In the earlier theoretical work, magneto-elastic coupling is suggested to contribute to the variation of the transition temperatures. This viewpoint is not contrary to the conclusion in this work. Instead, the origin of the in-plane magnetic anisotropy may be attributed to the magneto-elastic interaction, as experimentally revealed in some other materials [37, 38]. Thus, it is suggested here that such a mechanism may also work in the iron pnictides such as $BaFe_2As_2$ [39]. Furthermore, no obvious dependence of the values of T_S-T_N on either A_J or A_t is observed, consistent with our earlier conclusion that the formation of the nematic order is almost independent of the exchange anisotropy [23].

Most recently, the interchange between the FM and AFM directions has been predicted in the density functional theory calculations when the sign of the orthorhombicity is changed at a critical uniaxial stress in $BaFe_2As_2$ [17]. In the present work, this phenomenon is also studied based on the fact that the sign of A_J may change with the predicted orthorhombicity jump. In addition, it is expected from the symmetries of the model Hamiltonian that the sign change of A_J should generate a 90 degree rotation of the collinear AFM order. This viewpoint has been confirmed in our simulation. The simulated results for various negative A_J at $A_t = 0$ are presented in figure 4. At the transition point, (~116 K for $A_J = -0.14$), the spin structure factor $\Phi(0, \pi)$ increases (figure 4(a)) while $\Phi(\pi, 0)$ remains small (not shown here), indicating the development of the $(0, \pi)$ AFM order. Thus, in our simulation, the replacement of the $(\pi, 0)$ AFM order by $(0, \pi)$ is observed when the sign of A_J is changed. In addition, both the $(0, \pi)$ AFM and nematic orders are enhanced by negative A_J, resulting in the increases of T_N and T_S as the magnitude of A_J increases, as indicated by the results of the magnetic and nematic susceptibilities given in figures 4(b) and (d), respectively. Furthermore, figure 5 shows the calculated phase diagram for negative A_J, which also exhibits an obvious region with the nematic order in the absence of the long range AFM one.

On the other hand, the occupancies of the three orbitals at the Fermi surface in the AFM states are also investigated in our simulation. Figure 6(a) shows the orbitally resolved electronic density of states DOS(ω) for the perfect $(\pi, 0)$ AFM order. Here, the well-known twisted boundary conditions are used to reduce finite size effects in the measurement, and the number of possible momenta in the FM or AFM directions is selected to be 256 [40, 41]. Similarly to previous findings, the $(\pi, 0)$ AFM order opens a pseudogap in the d_{yz} orbital, and the d_{xz} orbital is dominant at the Fermi level (ω equals chemical potential μ) [21]. Actually, this interesting property is suggested to be essential in the understanding of the transport anisotropy between the FM and AFM directions

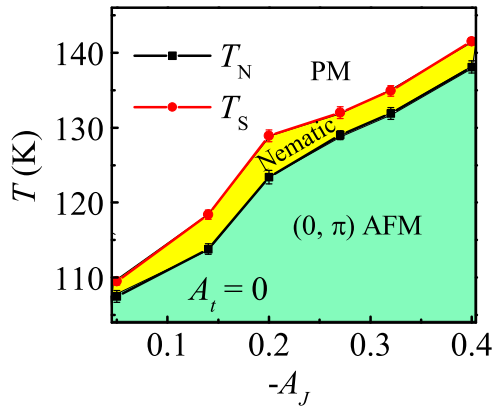

Figure 5. The phase diagram in the (A_J, T) plane at $A_t = 0$ for $A_J < 0$.

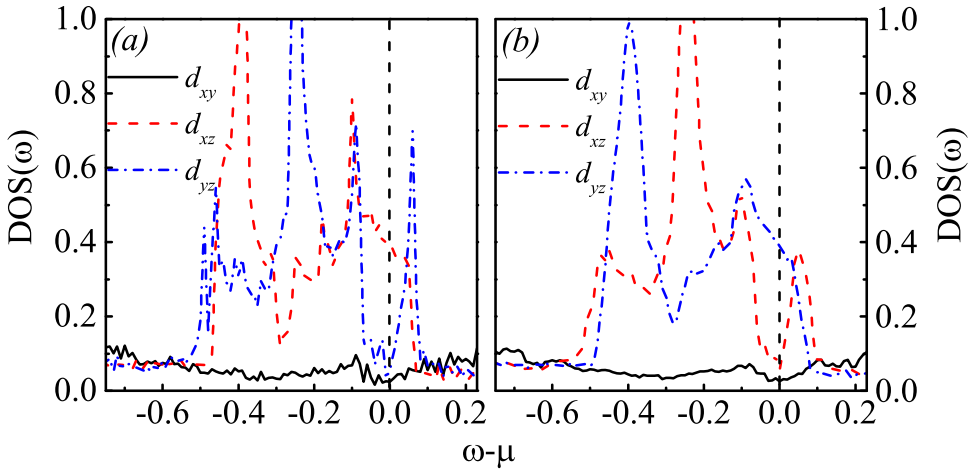

Figure 6. Density of states DOS(ω) of each orbital for the perfect (a) (π, 0) AFM order, and (b) (0, π) AFM order.

in pnictide superconductors due to the fact that the d_{xz} Fermi surface population favors transport along the AFM bonds (x axis in figure 1(a)) [21]. Figure 6(b) shows the calculated DOS(ω) for the (0, π) AFM order, which clearly demonstrates that the d_{yz} orbital is dominant at the Fermi surface. Thus, our simulations show that the ferro d_{xz} Fermi surface orbital order can be stabilized for the (π, 0) AFM order at low T under positive A_J, while the ferro d_{yz} one can be developed for the (0, π) AFM order under negative A_J. In other words, the orbital occupations d_{xz} and d_{yz} at the Fermi surface are reversed when the sign of A_J is changed, which is compatible with earlier theoretical prediction [17].

4. Conclusion

In summary, we investigated strain effects on the phase transitions in $BaFe_2As_2$ by the Monte Carlo simulation of the undoped three-orbital spin-fermion model taking into account the superexchange and Fe–Fe hopping anisotropies. Both the collinear antiferromagnetic and nematic transition temperatures increase as the magnitude of the anisotropies increases, qualitatively agreeing with the experimental results. Thus, our simulations indicate that both anisotropic superexchange and Fe–Fe hopping may contribute to the variation of the transition temperatures of $BaFe_2As_2$ with uniaxial stress. Furthermore, the reversal of the orbital occupancy at the Fermi surface and the switch between the ferromagnetic and antiferromagnetic directions are observed when the sign of the superexchange anisotropy changes, compatible with the earlier prediction by the first principles calculation.

Acknowledgments

The authors acknowledge C-S Ting for fruitful discussions. The work performed at University of Houston is funded by the Texas Center for Superconductivity of the University of Houston (TcSUH), and the work performed in China is supported by the funds of NSFC(11204091, 51322206, 11274094, 51332007), and NBRPC (2015CB921202, 2011CB922101).

References

[1] Stewart G R 2011 *Rev. Mod. Phys.* **83** 1589
[2] Dai P C, Hu J P and Dagotto E 2012 *Nat. Phys.* **8** 709
[3] Dagotto E 2013 *Rev. Mod. Phys.* **85** 849
[4] Chuang T M, Allan M P, Lee J, Xie Y, Ni N, Budko S L, Boebinger G S, Canfield P C and Davis J C 2010 *Science* **327** 181
[5] Kasahara S *et al* 2012 *Nature* **486** 382
[6] Xu C, Muller M and Sachdev S 2008 *Phys. Rev.* B **78** 020501 (R)
[7] Fernandes R M, Chubukov A V, Knolle J, Eremin I and Schmalian J 2012 *Phys. Rev.* B **85** 024534
[8] Lu X Y, Park J T, Zhang R, Luo H Q, Nevidomskyy A H, Si Q M and Dai P C 2014 *Science* **345** 657
[9] Fang C, Yao H, Tsai W F, Hu J P and Kivelson S A 2008 *Phys. Rev.* B **77** 224509
[10] Wysocki A L, Belashchenko K D and Antropov V P 2011 *Nat. Phys.* **7** 485
[11] Fernandes R M, Chubukov A V and Schmalian J 2014 *Nat. Phys.* **10** 97
[12] Dhital C, Yamani Z, Tian W, Zeretsky J, Sefat A S, Wang Z Q, Birgeneau R J and Wilson S D 2012 *Phys. Rev. Lett.* **108** 087001
[13] Blomberg E C *et al* 2012 *Phys. Rev.* B **85** 144509
[14] Dhital C, Hogan T, Yamani Z, Birgeneau R J, Tian W, Matsuda M, Sefat A S, Wang Z Q and Wilson S D 2014 *Phys. Rev.* B **89** 214404
[15] Cano A and Paul I 2012 *Phys. Rev.* B **85** 155133
[16] Hu J P, Setty C and Kivelson S 2012 *Phys. Rev.* B **85** 100507 (R)
[17] Tomic M, Jeschke H O, Fernandes R M and Valenti R 2013 *Phys. Rev.* B **87** 174503
[18] Chu J H, Analytis J G, Greve K D, McMahon P L, Islam Z, Yamamoto Y and Fisher I R 2010 *Science* **329** 824
[19] Yin W G, Lee C C and Ku W 2010 *Phys. Rev. Lett.* **105** 107004
[20] Lv W C, Kruger F and Phillips P 2010 *Phys. Rev.* B **82** 045125
[21] Liang S H, Alvarez G, Sen C, Moreo A and Dagotto E 2012 *Phys. Rev. Lett.* **109** 047001
[22] Liang S H, Moreo A and Dagotto E 2013 *Phys. Rev. Lett.* **111** 047004
[23] Qin M H, Dong S, Zhao H B, Wang Y, Liu J-M and Ren Z F 2014 *New J. Phys.* **16** 053027
[24] Dagotto E, Hotta T and Moreo A 2001 *Phys. Rep.* **344** 1
[25] Dong S, Yunoki S, Zhang X T, Sen C, Liu J-M and Dagotto E 2010 *Phys. Rev.* B **82** 035118
[26] Zhao J, Ratcliff W, Lynn J W, Chen G F, Luo J L, Wang N L, Hu J P and Dai P C 2008 *Phys. Rev.* B **78** 140504 (R)
[27] Zhao J, Adroja D T, Yao D X, Bewley R, Li S L, Wang X F, Wu G, Chen X H, Hu J P and Dai P C 2009 *Nat. Phys.* **5** 555
[28] Hu J P, Xu B, Liu W M, Hao N N and Wang Y P 2012 *Phys. Rev.* B **85** 144403
[29] Hu J P and Xu C K 2012 *Physica* C **481** 215
[30] Daghofer M, Nicholson A, Moreo A and Dagotto E 2010 *Phys. Rev.* B **81** 014511
[31] Glasbrenner J K, Velev J P and Mazin I I 2014 *Phys. Rev.* B **89** 064509
[32] Calderon M J, Valenzuela B and Bascones E 2009 *Phys. Rev.* B **80** 094531
[33] Dong S, Yu R, Yunoki S, Liu J-M and Dagotto E 2008 *Phys. Rev.* B **78** 064414
[34] Fernandes R M and Schmalian J 2012 *Supercond. Sci. Technol.* **25** 084005
[35] Wang H Y 2012 *Phys. Rev.* B **86** 144411
[36] Dong S, Yu R, Liu J-M and Dagotto E 2009 *Phys. Rev. Lett.* **103** 107204
[37] Fan Y, Zhao H B, Lupke G, Hanbicki A T, Li C H and Jonker B T 2012 *Phys. Rev.* B **85** 165311
[38] Pandey H, Rout P K, Guleria A, Joshi P C, Hossain Z and Budhani R C 2014 *Appl. Phys. Lett.* **104** 022402
[39] Kawaguchi T, Sakagami A, Mori Y, Tabuchi M, Ujihara T, Takeda Y and Ikuta H 2014 *Supercond. Sci. Technol.* **27** 065005
[40] Salafranca J, Alvarez G and Dagotto E 2009 *Phys. Rev.* B **80** 155133
[41] Liang S H, Mukherjee A, Patel N D, Bishop C B, Dagotto E and Moreo A 2014 *Phys. Rev.* B **90** 184507